Sequence-Selective DNA Binding by Linked Bis-*N*-methylpyrrole Dipeptides: An Analysis by MPE Footprinting and Force Field Calculations†

K. Ekambareswara Rao, Jürg Zimmermann, and J. William Lown*

Department of Chemistry, University of Alberta, Edmonton, Alberta, Canada T6G 2G2

Received March 12, 1990

The binding of a series of linked bis-oligopeptides, designed to examine the phasing problem of the molecular recognition by longer ligands of DNA sequences, was examined by MPE complementary strand footprinting on a EcoRI/HindIII restriction fragment of pBR322 DNA. Ligands bearing *N*-methylpyrrole dipeptide moieities linked by trans olefinic or trans 1,2-cycloalkane moieties (n = 3, 4, 5, 6) give evidence of bidentate binding in $(AT)_n$ rich sequences from footprinting at r' = 0.16. By contrast those ligands linked by cis olefinic or cis 1,2-cyclopropane tethers exhibit monodentate binding. These results on the relative binding of cis and trans isomeric ligands are corroborated by detailed studies employing ultraviolet and circular dichroism spectroscopic studies on representative pairs of compounds which permit, inter alia, the determination of binding parameters, stoichiometry, and association constants. Consideration of the energetics of binding of cis–trans pairs of ligands suggests operational rather than true bidentate binding of the trans compounds via a "dancing" mode. The influence of ligand conformation and other structural parameters on the efficiency of drug binding was examined by a detailed force field analysis employing the MMX program. These calculations permitted the interpretation of the experimental data and comparison with "ideal" minor groove binders.

Introduction

One approach to the general problem of developing DNA sequence specific ligands for possible application in genetic targeting[1] is by modifying lead compounds derived from natural products or synthetic DNA binding agents. Groove-selective binding agents have several advantages over intercalators for this purpose in that, unlike the latter, groove binders normally cause minimal structural distortion of the DNA and, correspondingly, less interference with the reading of information inherent in the DNA sequence.[2] We have reported a promising approach for this purpose based on the naturally occurring oligopeptide antitumor antibiotics netropsin 1 and distamycin 2.[3,4] Rational structural modification led to the development of lexitropsins, or information reading molecules, some of which are capable of recognizing unique sequences different from those of the parent antibiotics.[5-9] Additional advantagous properties of these oligopeptides include ready access into cells and concentration in the nucleus.[10] Systematic studies have permitted the identification of several structural,[5,6] stereochemical,[7,9] and other physical[11-13] factors which contribute to the overall molecular recognition process.

One of the central problems in targeting relatively longer segments of DNA [15 to 16 base pairs defines a unique sequence in the human genome[14]] concerns the repeat distance of a nucleotide unit of DNA and the hydrogen bond and van der Waals contacts generated by oligopeptidic lexitropsins. This problem is sometimes referred to as the phasing problem.[5,16] In model studies involving idealized B-DNA coordinates it was demonstrated that as the netropsin-like ligand increases in length, the hydrogen bond contacts and van der Waals contacts between the ligand and DNA become seriously out of phase with the spacing between the nucleotide units of DNA.[15] This phenomenon may explain the reduced binding affinities exhibited by certain poly-*N*-methylpyrrole peptides.[17,18]

An initial approach to this problem is to connect the *N*-methylpyrrole dipeptide moieties by a suitable tether.[19-22] We recently described such structures incorporating variable-length, flexible and rigid tethers between two netropsin-like moieties.[23] Footprinting evidence

†This investigation was supported by grants (to J.W.L.) from the Medical Research Council of Canada and the Natural Sciences and Engineering Research Council of Canada.

(1) (a) Caruthers, M. H. *Acc. Chem. Res.* **1980**, *13*, 155. (b) Frederick, C. A.; Grable, J.; Melia, M.; Samudzi, C.; Jen-Jacobson, L.; Wang, B. C.; Greene, P.; Boyer, H. W.; Rosenberg, J. W. *Nature* **1984**, *309*, 327. (c) Gurskii, G. V.; Tumanyan, V. G.; Zavedatelev, A. S.; Zhyze, A. L.; Grokhovsky, S. L.; Gottikhi, B. P. In *Nucleic Acid–Protein Recognition*; Vogel, J. J., Ed.; Academic Press: New York, 1977; p 189. (d) Kim, S. H.; Sussman, J. L.; Church, G. M. In *Structure and Conformation of Nucleic Acids and Protein–Nucleic Acid Interactions*; Sundaralingam, M., Rao, S. T., Eds.; University Park Press: Baltimore, MD, 1974; pp 571–575. (e) Takeda, Y.; Ohelndorf, D. H.; Anderson, W. F.; Matthews, B. W. *Science* **1983**, *221*, 1020.

(2) Kopka, M. L.; Yoon, C.; Goodsell, D.; Pjura, P.; Dickerson, R. E. *J. Mol. Biol.* **1985**, *183*, 553.

(3) Lown, J. W. *Anti-Cancer Drug Design* **1988**, *3*, 25.

(4) Lown, J. W. *Org. Prep. Proc. Int.* **1989**, *21*, 1.

(5) Lown, J. W.; Krowicki, K.; Bhat, U. G.; Skorobogaty, A.; Ward, B.; Dabrowiak, J. C. *Biochemistry* **1986**, *25*, 7408.

(6) Kissinger, K.; Krowicki, K.; Dabrowiak, J. C.; Lown, J. W. *Biochemistry* **1987**, *26*, 5590.

(7) Lee, M.; Shea, R. G.; Hartley, J. A.; Kissinger, K.; Vesnaver, G.; Breslauer, K. J.; Pon, R. T.; Dabrowiak, J. C.; Lown, J. W. *J. Mol. Recogn.* **1989**, *2*, 6.

(8) Lee, M.; Chang, D. K.; Hartley, J. A.; Pon, R. T.; Krowicki, K.; Lown, J. W. *Biochemistry* **1988**, *27*, 445.

(9) Lee, M.; Shea, R. G.; Hartley, J. A.; Kissinger, K.; Pon, R. T.; Vesnaver, G.; Bresslauer, K. J.; Dabrowiak, J. C.; Lown, J. W. *J. Am. Chem. Soc.* **1989**, *111*, 345. (b) Lee, M.; Krowicki, K.; Hartley, J. A.; Pon, R. T.; Lown, J. W. *J. Am. Chem. Soc.* **1988**, *110*, 3641.

(10) Bailly, C.; Catteau, J. Q.; Henichart, J. P.; Reszka, K.; Shea, R. G.; Krowicki, K.; Lown, J. W. *Biochem. Pharmacol.* **1989**, *38*, 1625.

(11) Pullman, A.; Pullman, B. *Int. Rev. Biophys.* **1981**, *14*, 289.

(12) Lavery, R.; Pullman, B. *J. Biomol. Struct. Dyn.* **1985**, *2*, 1021.

(13) Lavery, R.; Pullman, B.; Pullman, A. *Theor. Chim. Acta* **1982**, *62*, 93.

(14) Helene, C. Lecture on Antisense Probes in the International Symposium on DNA as a Target for Chemotherapeutic Action, Seillac, France, October 11–15, 1987.

(15) Kissinger, K. L.; Dabrowiak, J. C.; Lown, J. W. *Chem. Res. Toxicol.* **1990**, *3*, 162.

(16) Goodsell, D.; Dickerson, R. E. *J. Med. Chem.* **1986**, *29*, 727.

(17) Youngquist, R. S.; Dervan, P. B. *Proc. Natl. Acad. Sci. U.S.A.* **1985**, *82*, 2565.

(18) Luck, G.; Zimmer, C.; Reinert, K. E.; Arcamone, F. *Nucleic Acids Res.* **1977**, *4*, 2655.

(19) Kohrlin, A. A.; Krylov, A. S.; Grokhovsky, S. L.; Zhuze, A. L.; Zasedatelev, A. S.; Gursky, G. V.; Gottikh, B. P. *FEBS Lett.* **1980**, *118*, 311.

(20) Gursky, G. V.; Zasedatelev, A. S.; Zhuze, A. L.; Khorlin, A. A.; Grokhovsky, S. L.; Streltsov, S. A.; Surovaya, A. N.; Nikitin, S. M.; Krylov, A. S.; Retchinsky, V. O.; Michailov, M. V.; Beabealashvili, R. S.; Gottikh, B. P. *Cold Spring Harbor Symp. Quant. Biol.* **1983**, *47*, 367.

(21) Youngquist, R. S.; Dervan, P. B. *J. Am. Chem. Soc.* **1985**, *107*, 5528.

(22) Schultz, P. G.; Dervan, P. B. *J. Am. Chem. Soc.* **1983**, *105*, 7748.

0022-3263/91/1956-0786$02.50/0 © 1991 American Chemical Society

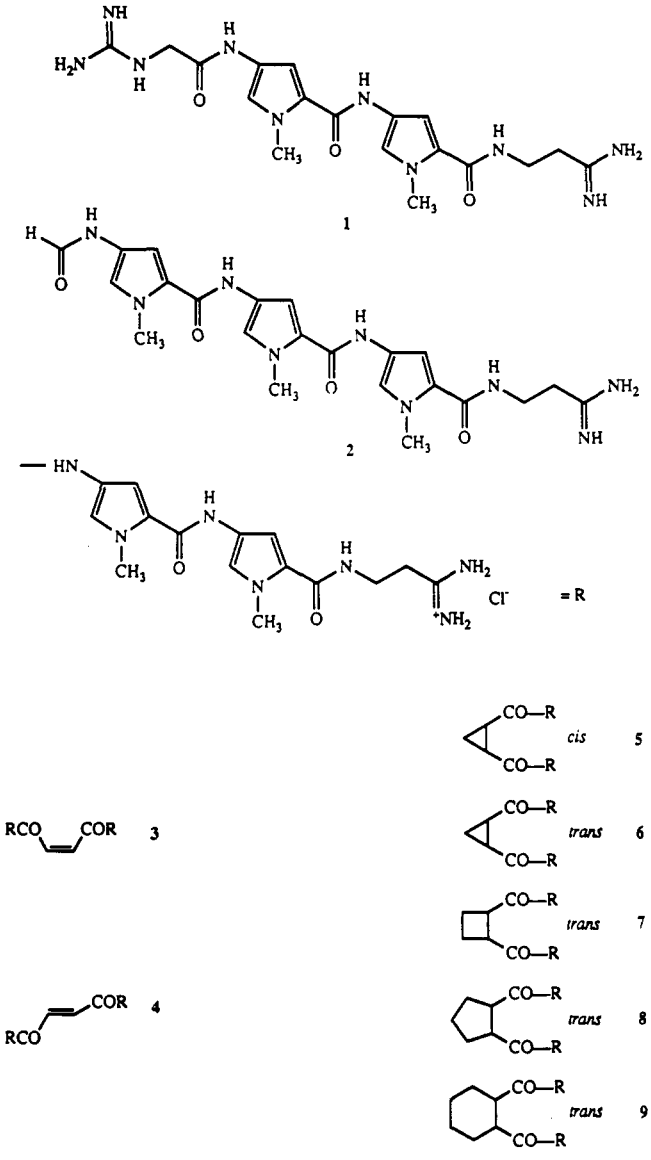

Figure 1. Structures of netropsin (1), distamycin (2), and the new linked bis-oligopeptides (3–9).

confirmed bidentate binding to 11 contiguous base pair sites for flexible polymethylene linkers beyond a minimum of $(CH_2)_3$.[15]

In the present study we focus on the effects of linker geometry and dihedral angle to the attached ligands, in cis and trans related cycloalkane and olefin-linked *N*-methylpyrrole dipeptides 3–9 (Figure 1) as a function of ring size and molecular geometry in determining bidentate versus monodentate DNA binding. The techniques employed include spectroscopic evaluation of binding and complementary strand MPE footprinting. A parallel investigation of the phase problem is described using molecular mechanics calculations.

Experimental Section

Chemicals and Biochemicals. Synthesis and characterization of compounds 3–9 (Figure 1) were reported recently.[24] The polynucleotide poly(dA-dT)·poly(dA-dT), pBR322 and sonicated calf thymus (ct) DNAs, restriction enzymes HindIII and EcoRI were obtained from Pharmacia P.L Biochemicals. All were used without further purification. Distamycin A HCl was obtained from Sigma. Ferrous ammonium sulfate was from BDH. The T_4 polynucleotide kinase, large fragment of DNA polymerase (Klenow fragment), Tris hydrochloride, and urea were from Bethesda Research Labs. Dithiothreitol (DTT) and calf intestine alkaline phosphatase (CAP) were obtained from Calbiochem. Acrylamide, bromophenol blue, and xylene cyanol were from Serva. γ-^{32}P-ATP and α-^{32}P-dATP were purchased from New England Nuclear. All other reagents were of analytical grade. Methidium propyl-EDTA (MPE) was a gift from Professor P. B. Dervan (Cal. Tech.).

The stock solutions of the compounds were prepared in the appropriate buffer. The concentrations of the ligands and DNAs are expressed in moles per liter. The concentrations of the ligands were determined spectrophotometrically by using $\epsilon_{298} = 3.56 \times 10^4$ M^{-1} (compound 6) and $\epsilon_{298} = 3.45 \times 10^4$ M^{-1} (compound 5). Concentration of poly(dA-dT) was measured by using $\epsilon_{260} = 6.7 \times 10^3$ M^{-1}. However, the new compounds were taken by weight for footprinting studies.

All experiments were carried out in aqueous solutions of 20 mM NaCl, pH 7.1, at 20 °C. r' is the input ratio of the concentration of ligand and polynucleotide (DNA).

Circular dichroism values are expressed as molar ellipticity $[\theta]$

$$[\theta] = \theta_{obs} \times 100/lc$$

where θ_{obs} = observed rotation, l = 0.5 cm, and c = molar concentration of poly(dA-dT) in nucleotide phosphates.

Determination of Binding Stoichiometry. The stoichiometry of binding of the new compounds to poly(dA-dT) was measured by monitoring the change in absorbance as a function of the ligand concentration in the presence of a fixed concentration of the polymer. A small volume of ligand containing the same concentration of poly(dA-dT) was added to the sample cuvette, and the absorbance was recorded at 300 and 316 nm. The difference in the absorbance at 300 and 316 nm was plotted against the concentration of the added ligand. The stoichiometry was determined from the break in the straight lines resulting from the plot. The ratio of the concentration of the ligand and poly(dA-dT) corresponding to the break point gives the stoichiometry value.[25]

Analysis of Binding Data. The binding parameters, intrinsic binding constant (K_o), and binding stoichiometry (r_b, number of ligand molecules bound per nucleotide base) were determined from the Scatchard equation on the basis of the assumption that an independent noncooperative type of binding takes place between the new ligands and poly(dA-dT)[26]

$$r/c_f = K_o(r_b - r)$$

(where $r = c_b/c_p$, c_b and c_p are the concentrations of the bound ligand and poly(dA-dT), respectively, and c_f is the concentration of the free ligand). A plot of r/c_f against r gives a straight line with intercepts r_b on the r axis, and k_a on the r/c_f axis, and slope $-K_o$. The experimental points were fitted by the method of least squares to obtain a straight line.

For the determination of c_b, the concentration of the bound ligand, a small aliquot of the ligand was added to the sample cuvette containing a fixed concentration of poly(dA-dT) (150–180 μM). The reference cuvette also contained the same concentration of the polynucleotide to take care of any possible contributions to absorbance from the polynucleotide.[27,28] However, the monitoring wavelength was chosen such that there was maximum change in absorbance of the ligand due to its binding to the polynucleotide and very little (or no) contribution from the absorbance by the DNA. The concentration of the bound ligand, c_b, corresponding to each titration point was calculated from the relation

$$c_b = \frac{(A_f - A_b)}{(\epsilon_f - \epsilon_b)}$$

where A_f and A_b are absorbance of free ligand and absorbance

(23) Lown, J. W.; Krowicki, K.; Balzarini, J.; Newman, R. A.; De Clercq, E. *J. Med. Chem.* **1989**, *32*, 2368.
(24) Rao, K. E.; Krowicki, K.; Balzarini, J.; De Clercq, E.; Newman, R. A.; Lown, J. W. *Eur. J. Med. Chem.*, in press.
(25) Povirk, L. F.; Dattagupta, N.; Warf, B. C.; Goldberg, I. H. *Biochemistry* **1981**, *20*, 4007.
(26) Scatchard, G. *Ann. N. Y. Acad. Sci.* **1949**, *51*, 660.
(27) Dasgupta, D.; Parrack, P.; Sasisekharan, V. *Biochemistry* **1987**, *26*, 6381.
(28) Rao, K. E.; Dasgupta, D.; Sasisekharan, V. *Biochemistry* **1988**, *27*, 3018.

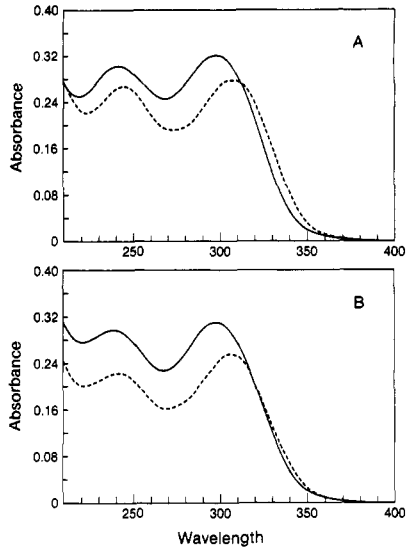

Figure 2. UV absorption spectra of (A) compound **6** (8.9 μM) and (B) compound **5** (8.9 μM) alone (—) and in the presence of poly(dA-dT) (---). The concentration of poly(dA-dT) was 50 μM in both cases.

of the ligand in the presence of poly(dA-dT), respectively. ϵ_f and ϵ_b are molar extinction coefficients of the free ligand and the bound ligand, respectively. ϵ_b was determined from the absorbance of the ligand in the presence of an 80-fold excess of poly(dA-dT).

MPE Complementary Strand Footprinting Procedures. EcoRI digested pBR322 DNA was labeled either at the 5′-end using γ-^{32}P-ATP, CAP, and T_4 kinase or at the 3′-end using α-^{32}P-dATP and the Klenow fragment. Then the resulting, either 5′- or 3′-labeled, fragments were digested with HindIII. The resulting 4332 and 31 base pair[29] fragments were not separated prior to the cleavage reactions. The footprinting reactions were carried out in the presence of sonicated calf thymus DNA, labeled DNA, and ligand (not present in the control) in 10 mM Tris, 20 mM NaCl buffer, pH 7.4. After equilibrating the ligand-DNA mixtures for 20 min at 37 °C, DTT, and MPE·Fe(II) (made freshly) were added to each reaction tube. The final reaction mixtures contained 100 μM DNA, 10 mM Tris, 20 mM NaCl, 10 μM MPE·Fe(II), 2.5 mM DTT, and 8, 16, 32, 48, or 78 μM of ligand. Reactions were run at room temperature for 15 min and then stopped by freezing at −70 °C. The solutions were then lyophilized and resuspended in formamide loading buffer[30] for gel electrophoresis. The reaction mixtures were analyzed on 0.4 mm thick, 55 cm long, 6% polyacrylamide and 7 M urea denaturing gels at 1900 V and 55 °C. Then the gels were transferred onto a filter paper and dried on a Bio-Rad Model 483 slab dryer. The gels were then autoradiographed at −70 °C using Kodak X-Omat AR film.

The densitometric data were corrected for the background absorbance of the film (<0.3 absorbance). In order to compensate for possible variations in extent of reaction, all band intensities within a lane were normalized to a band which is unaffected in the presence of compound in that lane. The extent of protection from cleavage for each base was determined by

$$\% \text{ protection} = [1 - (A_{L+D}/A_D)]100$$

where A_{L+D} is the absorbance of a band obtained from cleavage in the presence of added ligand and A_D is the absorbance of the same band in the absence of ligand (control lane). Negative values for protection correspond to cleavage enhancement in the presence of the ligand.

Molecular Modeling. The force field and π calculations were carried out using the program MMX, version PC MODEL. Distances as a function of dihedral angles were computed with MacMOMO which was run on an Macintosh Plus.

(29) Peden, K. W. C. *Gene* **1983**, *22*, 277.
(30) Maniatis, T.; Fritsh, E. F.; Sambrook, J. *Molecular Cloning (A Laboratory Manual)*; Cold Spring Harbor Laboratory: Cold Spring Harbor, NY, 1982.

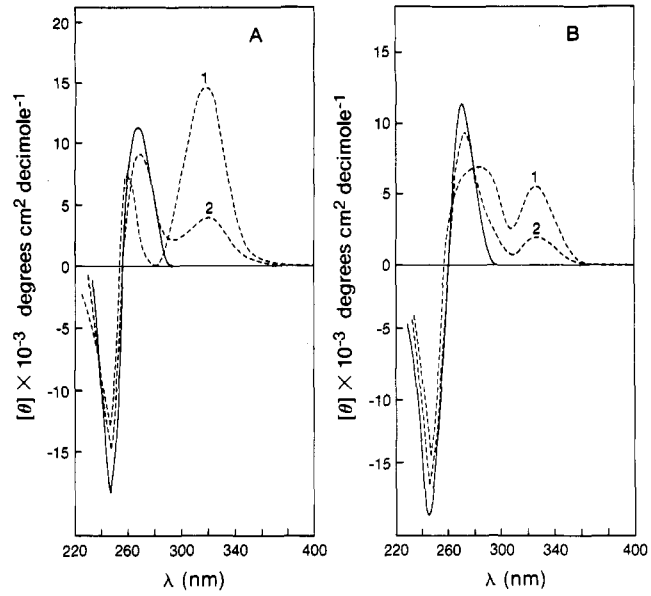

Figure 3. CD spectra of poly(dA-dT) in the absence (---) and presence (—) of (A) compound **6** at 0.05 (1) and 0.02 (2) ratios and (B) compound **5** at 0.05 (1) and 0.02 (2) ratios. The concentration of poly(dA-dT) was 185 and 210 μM in Figures A and B, respectively.

Results of DNA Binding and Spectroscopic Studies. Absorption Spectra of the Ligand–Poly(dA-dT) Complexes. The UV absorption spectra of the ligands are shown in Figure 2. Both compounds **5** and **6** have peaks at 240 and 298 nm. The position and intensity of the long wavelength peak is comparable to the Dst peak, which depends on the number of pyrrole rings.[27]

The binding of the two ligands to poly(dA-dT) is evident from the change in the UV absorption spectra of the free ligands in the presence of the polymer. The absorption spectra of the free ligands and in the presence of poly(dA-dT) are shown in Figure 2. The spectrum of the ligand (in each case) undergoes a red shift on complexation with poly(dA-dT) and also a hypochromic effect is associated with complexation. The extent of the red shift in the case of compound **6** is about 12 nm and in the case of compound **5** is 10 nm relative to the 298 nm peak of the free ligands. A red shift of about 12 nm and 15–16 nm was reported for Nt and Dst, respectively.[27] Both compounds exhibit isosbestic points for the complexes up to an input ratio, r', of 0.11 and 0.17 for compounds **6** and **5**, respectively. This may indicate a single mode of binding up to those ratios. The peak at 240 nm is not shifted significantly upon complexation with DNA in either of the cases. The UV absorption spectra indicated both cis and trans bis compounds interact similarly with poly(dA-dT) except that the latter saturates the polymer at lower r' ratios than the former.

CD Spectra of Ligand–Poly(dA-dT) Complexes. The binding of compounds **5** and **6** to poly(dA-dT) is further supported by the presence of an induced Cotton band in the 350–300-nm region of the spectra of compound–poly(dA-dT) complexes (Figure 3). Neither compounds **5** nor **6** exhibit any CD band under the experimental conditions. Compound **6** shows an induced Cotton band with a peak at 320 nm. The position of the induced band is comparable with that of the Dst–poly(dA-dT) complex induced band. The complex of compound **5**–poly(dA-dT) has a distinct extrinsic band at 328 nm and a shoulder at 290 nm up to 0.04 ratio. At $r' \geq 0.05$ the shoulder (at lower ratios) at 290 nm is seen as a separate band. At higher ratios the complex of compound **5**–poly(dA-dT) gives two well-defined bands with maxima at 328 and 290 nm. The presence of two bands in the spectrum of the complex of compound **5**–poly(dA-dT) probably causes the band in the higher wavelength region to shift 8 nm toward the red region compared to the induced band (at 320 nm) of the complex of compound **6**–poly(dA-dT). Isobestic points are seen in both cases. The isosbestic point of the complex of compound **6**–poly(dA-dT) is at 292 nm while the complex of compound **5**–poly(dA-dT) exhibits an isosbestic point at 280 nm. This blue shift of 12 nm in the isosbestic point of complex of compound **6**–poly(dA-dT)

Table I. Summary of Spectroscopic Studies of the Binding of Ligands 5 and 6 to Poly(dA-dT)

compd	r_b			K_o,[c] M^{-1}	K_a,[c] M^{-1}	G,[d] kcal/mol
	a	*b*	*c*			
5	0.15	0.16	0.15	1.87×10^5	2.81×10^4	-5.96
6	0.09	0.10	0.09	6.78×10^5	6.10×10^4	-6.51
1[e]	-	-	0.13	2.00×10^6	2.60×10^5	-7.20
2[e]	-	-	0.14	2.80×10^6	3.80×10^5	-7.40

[a] From UV. [b] From CD. [c] From Scatchard plot. [d] From $\Delta G = -RT \ln K_a$. [e] From ref 22.

could be due to the presence of a band at 290 nm.

To confirm whether such a split in the induced band is characteristic of all the cis compounds, experiments were performed with a cis bis-*N*-methylpyrrole dipeptide compound wherein the two Nt moieties are linked by a maleic acid unit in compound 3. A similar band was observed at 280 nm above r' 0.15 (figure not shown). At lower ratios (up to r' 0.1) neither a band nor a shoulder is observed. There is no pronounced effect on the conservative spectrum of poly(dA-dT) upon complexation of compound 6. However, it is difficult to comment on the preservation of DNA structure in the case of the complex between compound 5 and poly(dA-dT) because of the presence of an induced band in DNA absorbance region.

Binding Stoichiometry for Ligand–Poly(dA-dT) Complexes. The binding stoichiometries were determined by UV (details given in the Experimental Section) and CD spectral titration methods. Determination of r_b by UV methods for the new compounds is shown in Figure 4a. The ratio of ligand to DNA at the break in the straight lines corresponds to the stoichiometry of the ligand (r_b). To determine the r_b from CD titration data the molar ellipticity at the maximum of the induced band is plotted against r'. Figure 4b illustrates the determination of ligand stoichiometry by this method.

The r_b values obtained in UV and CD methods are given in Table I. The r_b values obtained with the two methods are in good agreement, which indicates the validity of the r_b values obtained. The titration curve for compound 6 does not show a clear plateau as in the case of compound 5. This probably indicates a weak second mode of nonspecific binding. A similar phenomenon was reported earlier for Nt–poly(dA-dT) complex.[31] This may be an indication of interaction of both the charged ends of compound 6 with the polynucleotide as in the case of Nt.

The r_b values in Table I indicate that the polymer saturates at about one ligand molecule per 11 nucleotides in the case of compound 6 and one ligand molecule per about 6.5 nucleotides in the case of compound 5. These values explain why compound 6 saturates the polymer at lower concentrations. The r_b values in Table I indicate that compound 6 binds to longer sequences than does compound 5, a conclusion in accord with the footprinting results (vide infra). It appears that compound 6 binds to DNA with both the *N*-methylpyrrole dipeptide arms while compound 5 binds through one of the two netropsin arms and partial contacts of the linker.

Binding Constants for Ligand–Poly(dA-dT) Interaction. The binding constants were measured by the Scatchard procedure[26] as described under Materials and Methods. The method has been used assuming that the interaction between the ligands and poly(dA-dT) is of an independent noncooperative type. The linearity of the plots supports this assumption under the experimental conditions. The binding stoichiometry values of the new ligands evaluated by Scatchard plots are in good agreement with those values determined by UV and CD methods as described above.

Figure 5 shows the Scatchard plots for compounds 6 and 5. The intercept of the straight line on the r/c_f axis corresponds to the apparent association constant of the ligand for poly(dA-dT). The binding parameters obtained from Scatchard plots are given in Table I. For comparison the K_a values determined by the same method[27] for Nt and Dst are also shown in Table I.

It is apparent from the data that the K_a of compound 6 is double that of the value obtained for compound 5. This, together with the stoichiometry determination, imply that in the case of trans compound (6) both the bis-pyrrole arms of the compound are binding in some fashion to DNA (vide infra). The ΔG of the compounds for poly(dA-dT) are calculated from the relation $\Delta G = -RT \ln K_a$, where R and T are gas constant and absolute temperature, respectively, and K_a is the association constant of

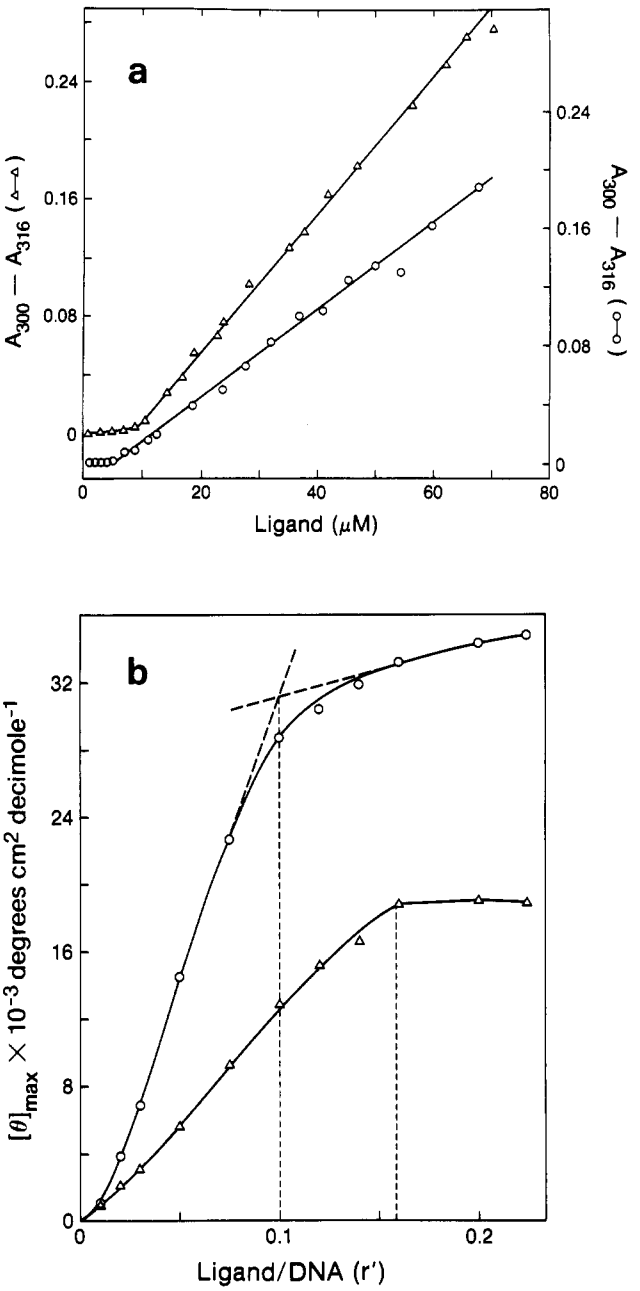

Figure 4. (a) Determination of the binding stoichiometries for ligand–poly(dA-dT) interaction. Plots of the difference in absorbances (at the wavelengths indicated) against the concentration of the compounds 6 (○) and 5 (△). Concentration of poly(dA-dT) in both the sample and reference cuvettes was 60 μM. r_b was measured from the plot as described under materials and methods. (b) Variation of the molar ellipticity [θ] with r'. Concentration of poly(dA-dT) was as described in Figure 3. r_b values were measured as described in text.

(31) Burckhardt, G.; Vatavova, H.; Sponar, J.; Luck, G.; Zimmer, Ch. *J. Bimol. Strutt. Dyn.* **1985**, 2, 721.

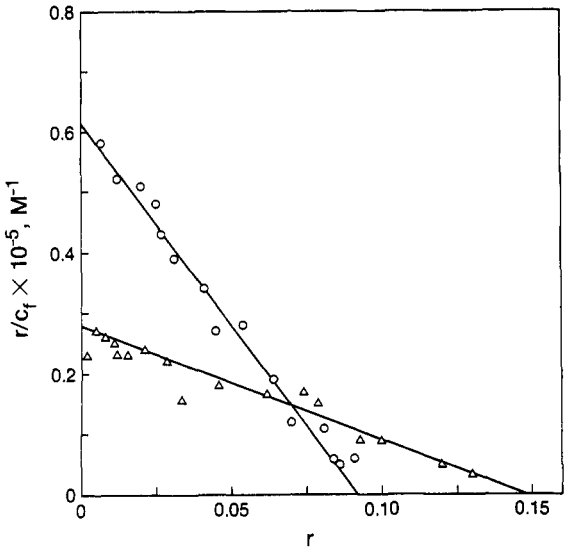

Figure 5. Scatchard plots of r/c_f against r for compounds **6** (○) and **5** (△). Determination of intrinsic binding constant, K_o, and binding stoichiometry, r_b, for the ligand–poly(dA-dT) is described under materials and methods.

the compound from Table I. The values are shown in Table I.

Footprinting Study of the Bis-*N*-methylpyrrole Dipeptides. Although the spectroscopic studies have concentrated on cis and trans cyclopropane linked compounds (**5** and **6**), footprinting studies were carried out on all the compounds **3–9**. The linker structure is varied from a rigid C=C through cyclopropane to a more flexible cyclohexane ring. The footprinting patterns of the new compounds on the 5′-labeled EcoRI/HindIII restriction fragment are shown in Figures 6 and 7. The areas of decreased intensity in the lanes containing compounds are due to protection from the MPE·Fe(II) cleavage by lexitropsins bound to the DNA fragment.

All the compounds bind to DNA. The footprints of this group of compounds are mainly located in four AT rich sites on the DNA fragment. The cleavage protection regions are (5′→3′) TTTAGAAAAATAAACAAATAG (4230–4250), CATTTG (4263–4268), GAAAAG (4272–4277), and TCTAAGAAACCATTATTATCA (4290–4310). It is difficult to assign exact binding sequences in the 4230–4250 base pair region owing to low resolution in the higher molecular weight region of the autoradiograms. Comparing the three isolated AT rich sequences at 4263–4268, 4272–4277, and 4290–4310 in this restriction fragment the latter AT stretch of bases proved suitable for examining monodentate versus bidentate binding of cis- and trans-linked compounds.

The strength of the footprints of the new compounds is comparable with that of distamycin footprints. However, the DNA binding pattern of cis linked compounds is different from those of the trans isomers. At higher r' values (>0.6) relatively little difference is observed in the footprinting patterns of the cis and trans bis-pyrrole dipeptides compared with distamycin, since at higher r' values all the compounds, including distamycin, give highly overlapped footprints. However, at $r' < 0.16$ the footprinting patterns of the cis compounds are very similar to that of the parent compound, distamycin, while the trans compounds give longer footprints than their cis congeners or distamycin. Figure 8 shows a summary of the footprinting patterns of the compounds at $r' = 0.78$ and 0.16 on the analyzed portion of the restriction fragment. At $r' = 0.78$ the footprints of all the compounds generally extend from nucleotides 4283–4313. At $r' = 0.16$ the footprints are confined largely to the region of nucleotides 4288–4310.

In Figure 9 the footprinting results obtained at $r' = 0.16$ are shown in the form of histograms. The binding sequences are assigned based on the positions of the maxima of the asymmetric inhibition pattern of the compounds on opposite strands.[32] However it is difficult to assign exactly the binding site boundaries based on this model.[21]

(32) Harshman, K. D.; Dervan, P. B. *Nucl. Acids Res.* **1985**, *13*, 4825.

Cis and Trans Olefinic Linkers (Compounds 3 and 4). The inhibition patterns of the two compounds are significantly different at lower r' values. In Figure 7 (lanes 3–8) it is seen that the inhibition pattern of cis compound (**3**) is very similar to the distamycin inhibition pattern (lanes 15–17 in Figure 7). The trans isomer (**4**) protects longer sequences on DNA.[15] Compound **3** (cis) protects nucleotides 4293–4298 and 4303–4308 as does distamycin. In contrast, the trans isomer (**4**) binds to the longer base sequence 4292–4308.

Cyclopropane Linker (Compounds 5 and 6). The footprinting patterns of the cis and trans cyclopropane linked compounds on 5′-end labeled DNA strand are seen in Figure 6 (lanes 9–14). As in the case of the olefinic linkers, the two congeners show different footprinting patterns. The cis compound, **5**, shows two distinct binding locations at 2493–4298 and 4303–4308 in the 4290–4310 base pair region at $r' = 0.16$. Again, in contrast, the trans compound, **6**, shows a longer footprint on nucleotides 4292–4308 in the same region.

Cyclobutane Linker (Compound 7). The footprinting pattern of this trans-linked compound are seen in Figure 6 (lanes 15–17). This compound also gives longer footprints similar to those of the cyclopropane-linked compound (**6**). The major footprint is located in the nucleotide region 4290–4310.

Cyclopentane and Cyclohexane Linkers (Compounds 8 and 9). These compounds represent more flexible linkers which, from the molecular mechanics analysis, are subject to greater conformational freedom. The footprints of these two compounds on 5′-end-labeled DNA strand are seen in Figure 6 (lanes 3–5 for compound **9** and lanes 6–8 for compound **8**). As in the case of other trans-linked compounds, these two compounds also give longer footprints. However, the strength of the footprints is lower compared with the footprints of the other more conformationally rigid trans compounds **4** and **7**.

The measured binding site size of the cis-linked ligands and distamycin is about 4–6 base pairs. The trans congeners cover about 5–9 base pairs per ligand molecule. According to the "n + 1 rule" (n is the number of amide hydrogens), true monodentate ligands like cis isomers should bind to 4 base pairs. The measured binding site size of 4–6 base pairs (spectroscopic study shows a binding site size of 6 base pairs for the cis cyclopropane linked compound, **5**) for cis isomers suggests that these compounds are binding to DNA in a monodentate fashion. Correspondingly, the trans congeners, subject to bindentate binding, should cover 7 base pairs. The measured binding site size of 7 + 1 base pairs is in good agreement with the predicted value. This suggests that the trans-linked compounds engage in effective bidentate binding with DNA. However, the slight deviation in the measured value for that predicted could be due to "dancing" of the ligands bound to the DNA, thereby constituting operational bidentate binding. In general the new compounds appear to tolerate occasional GC base pairs in a 6–9 base pair long binding sequence compared with the parent compound, distamycin, at least at the same r' (0.16).

Complementary strand analysis of MPE·Fe(II) footprinting shows the typical asymmetric shift of the footprints toward the 3′-end of the DNA with new compounds as does the parent compound, distamycin.[33] This indicates that the narrow groove of the right-handed B-DNA is the site of interaction for these compounds.[34] Adjacent to binding sites some enhanced cleavage of MPE·Fe(II) is observed with all the compounds.

Force Field Analysis: Molecular Mechanics Calculations. Five different structural, stereochemical, conformational, and energetical aspects have been examined for the alternative linkers. These are first described in terms of a hypothetical ideal linker.

Properties of an Ideal Tether Unit: (a) Linker Length. In order to match the distance of the consecutive base pairs on the floor of the minor groove, the repeat length between the amide hydrogens of the lexitropsin should be approximately 4.4 Å.[35] The tether unit in the "head-to-head" linked lexitropsins should therefore constrain the binding moieties so that the distance

(33) Van Dyke, M. W.; Dervan, P. B. *Cold Spring Harbor Symp. Quant. Biol.* **1982**, *47*, 347.

(34) Lane, J. M.; Vournakins, J. N.; Dabrowiak, J. C. *Prog. Clin. Biol. Res.* **1985**, *172*, 145.

(35) Kumar, S.; Zimmermann, J.; Yadagiri, B.; Pon, R. T.; Lown, J. W. *J. Biomol. Struct. Dyn.*, in press.

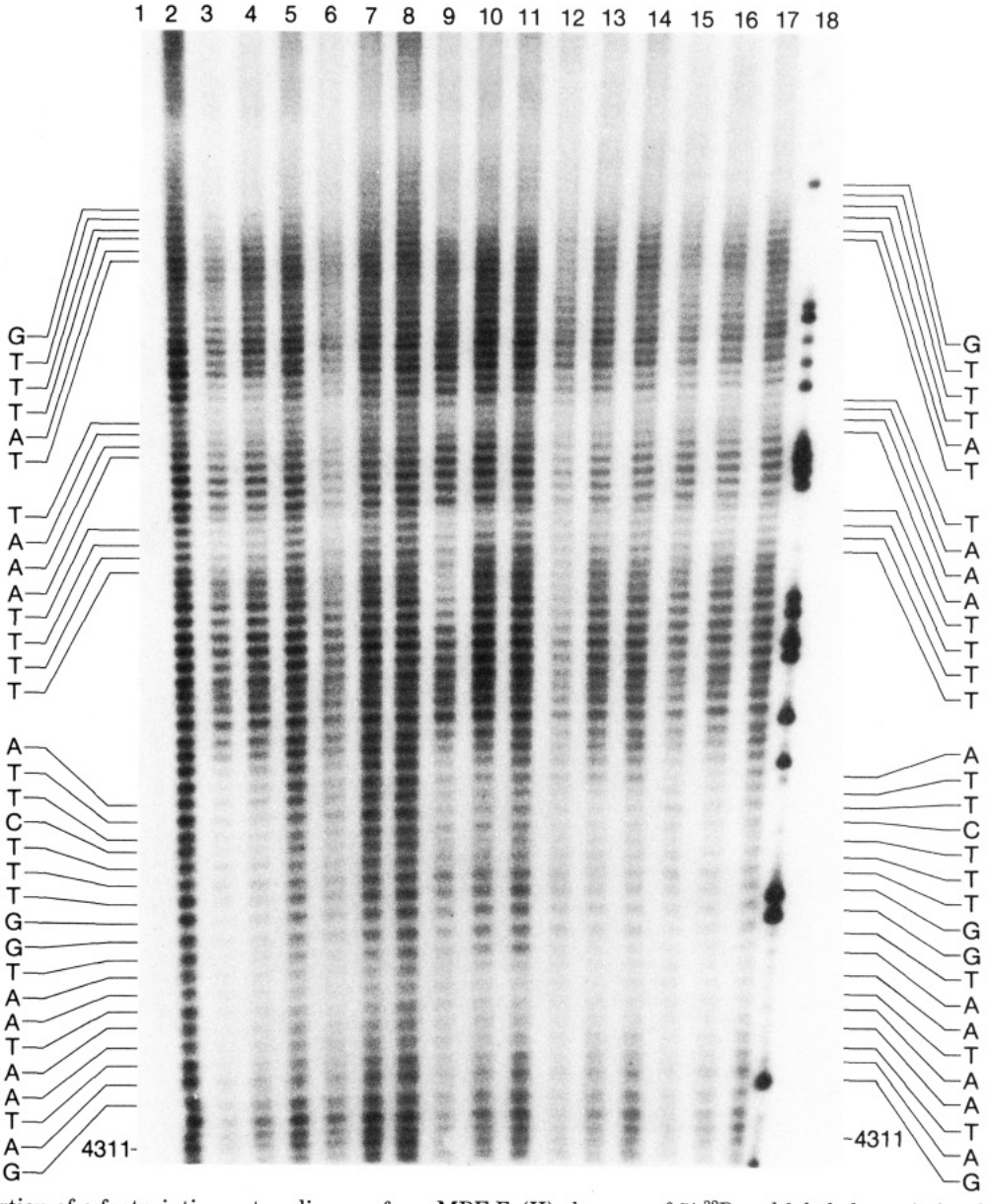

Figure 6. A portion of a footprinting autoradiogram from MPE·Fe(II) cleavage of 5′-^{32}P-end-labeled restriction fragment. Lane 1 contains intact DNA fragment. Lane 2 is control MPE·Fe(II) cleavage in the absence of ligand. Lanes 3, 6, 9, 12, and 15 contain ligands at 0.78 ratio. Lanes 4, 7, 10, 13, and 16 contain ligands at 0.39 ratio. Lanes 5, 8, 11, 14, and 17 contain ligands at 0.16 ratio. Lane 18 is Maxam–Gilbert sequencing "G" reaction. Lanes 3–5, 6–8, 9–11, 12–14, and 15–17 contain compounds **9**, **8**, **5**, **6**, and **7**, respectively.

between the amide hydrogens is ca. 4.4 Å or a multiple of it (Figure 10a).

(b) Flexibility of the Linker Length. From X-ray data[36] and MM2 calculations[37] it is known that, for example, pyrrole and 2-aminothiazole-5-carboxylate units are too wide to match perfectly the base pairs in the minor groove. In contrast lexitropsins bearing thiazole units with the nitrogen directed toward the floor of the minor groove are too short. An ideal tether would thus be capable of compensating for either too long or too short a ligand unit so as to bring an adjacent lexitropsin moiety back into phase with the base pairs of the DNA (Figure 10b).

(c) Correct Shape. Minor groove ligands bind isohelically to B-DNA.[16] Therefore, the tether unit should not interfere with the required crescent-shaped conformation of a suitable ligand (Figure 10c).

(d) Stability of the Required Conformation. The most stable conformation of an ideal tether-linked ligand will already be appropriate for binding to DNA. If, however, the required conformation for binding is not the most stable one, the kinetic and thermodynamic parameters of the binding process become less favorable (Figure 11a,b).

(e) Rigidity of the Linker. The binding process of potentially bidentate (or multidentate) ligands probably begins with the attraction of a positively charged terminal group to the DNA followed by anchoring to the floor of the minor groove. The rest of the ligand is then constrained to nestle within the adjacent sections of the groove. If the linker unit is not rigid the remaining portion of the ligand may remain in solution, or else engage in a "dancing" mechanism of two site exchange in which the bound and unbound moieties exchange their roles rapidly. This could give rise to operational or effectively time-averaged bidentate binding which may prove to be as effective as "true" bidentate binding for biological purposes (Figure 10d). On the other hand firm bidentate binding which results from a rigid tether may interfere with, or lessen, sequence selectivity. This is because, following the initial molecular recognition and binding, and effective local concentration of the adjoining ligand group is increased so as to promote binding of the second group.

Procedures for Molecular Mechanics Calculations. In screening the suitability of different linkers, the following procedure was adopted. (i) The individual extended tether molecule

(36) Pjura, P.; Grzeskowiak, K.; Dickerson, R. E. *J. Mol. Biol.* **1987**, *197*, 257.

(37) Kumar, S.; Jaseja, M.; Zimmermann, J.; Yadagiri, B.; Pon, R. T.; Sapse, A. M.; Lown, J. W. *J. Biomol. Struct. Dyn.* **1990**, *8*, 99.

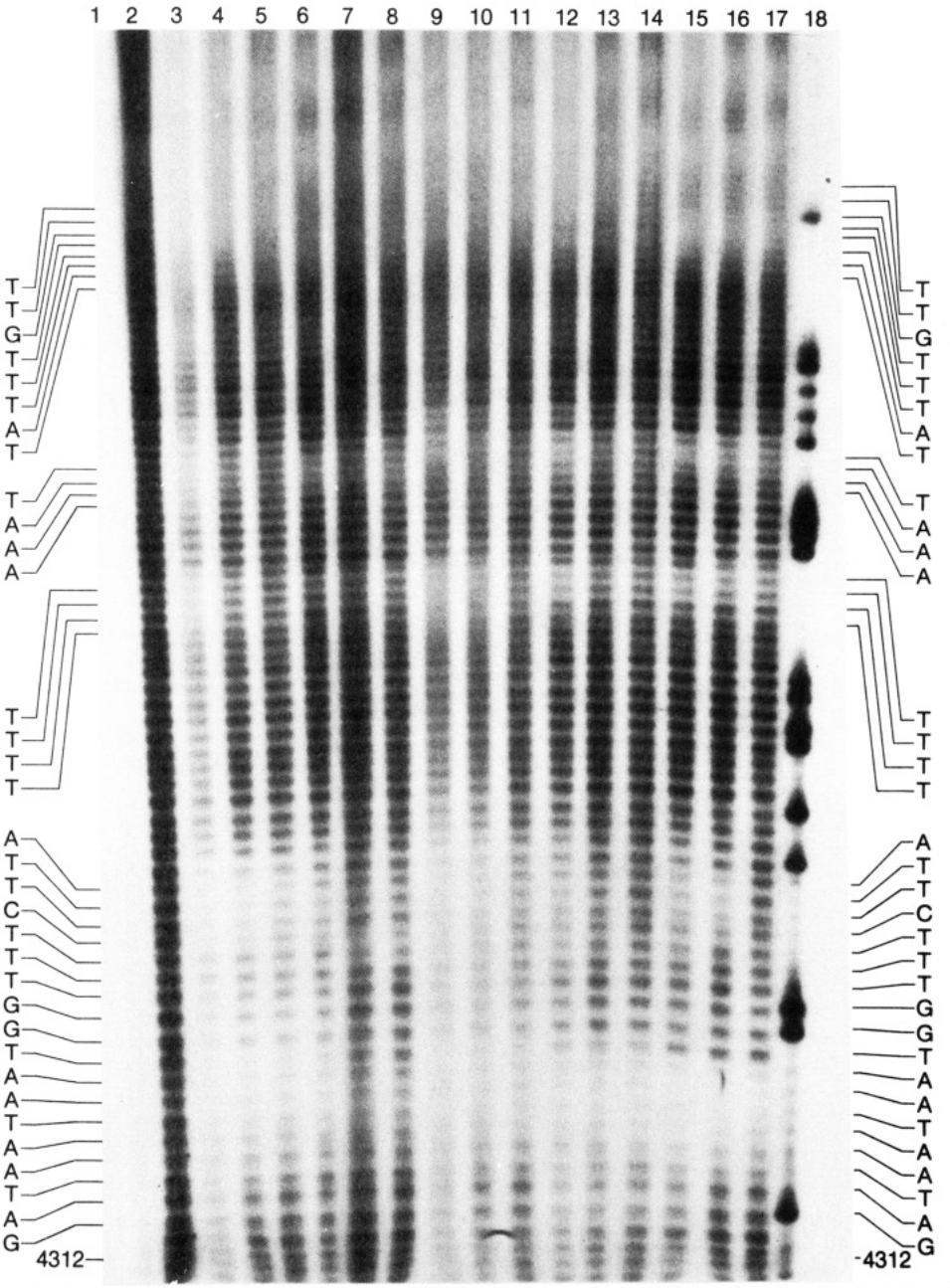

Figure 7. A portion of a footprinting autoradiogram from MPE·Fe(II) cleavage of 5′-^{32}P-end-labeled restriction fragment. Lane 1 contains intact DNA fragment. Lane 2 is control MPE·Fe(II) cleavage in the absence of ligand. Lanes 3, 6, 9, 12, and 15 contain ligands at 0.78 ratio. Lanes 4, 7, 10, 13 and 16 contain ligands at 0.39 ratio. Lanes 5, 8, 11, 14, and 17 contain ligands at 0.16 ratio. Lane 18 is Maxam–Gilbert sequencing "G" reaction. Lanes 3–5, 6–8, and 15–17 contain compounds **4**, **3**, and **2**, respectively. Disregard lanes 9–14.

was energy minimized using MM2,[38] thereby obtaining the most stable conformation. (ii) The coordinates of this most stable conformation were fed into the program MacMOMO. The repeat length l was calculated as a function of the torsion angles $\zeta 1$ and $\zeta 2$ (Figure 11c). The resulting data were then represented in a conformational plot. The contour lines represent identical repeat lengths. (iii) Those conformations with the correct repeat length l (4.4 ± 0.8 Å) were verified using molecular models. The head-to-head linked lexitropsin binding units must run in opposite directions and both of the hydrogen atoms on the amide groups must face in the same direction. Considerable variation of the repeat length can be seen in the conformation plot. The closer the contour lines (the steeper the slope) the better the tether can adjust the distance without changing the conformation of the ligand to any great extent. (iv) The energy of the conformations, which passed tests i–iii, was calculated by MM2. The resulting total strain energy was compared with that of the most stable conformation derived from i above.

Force Field Analyses for Bis-*N*-methylpyrrole Dipeptides. Trans Cyclopropane Linker. The conformation plots (Figure 12a) indicate several different conformations with the desired linker length. Within these areas, the conformations with the required spatial arrangement are indicated in Figure 12a. It should be noted however that none of these conformations fits precisely into the minor groove in that the geometry has to be adjusted slightly through rotation around the neighboring single bonds. It is also noteworthy that the conformation deduced for optimal bidentate binding in the minor groove resembles the heterocyclic units of the lexitropsins themselves (Figure 12b). Furthermore the conformation plot indicates considerable flexibility of the linker length for these conformations. A change of torsional angle of 30–40° causes a change in the linker length of approximately

(38) Osawa, E.; Musso, H. Application of Molecular Mechanics Calculations in Organic Chemistry. In *Topics of Stereochemistry*; Allinger, N. L., Eliel, E. L., Wilen, S. H., Eds.; Wiley: New York, 1982; p 117. Burket, U.; Allinger, N. L. *Molecular Mechanics*; American Chemical Society: Washington, DC, 1982.

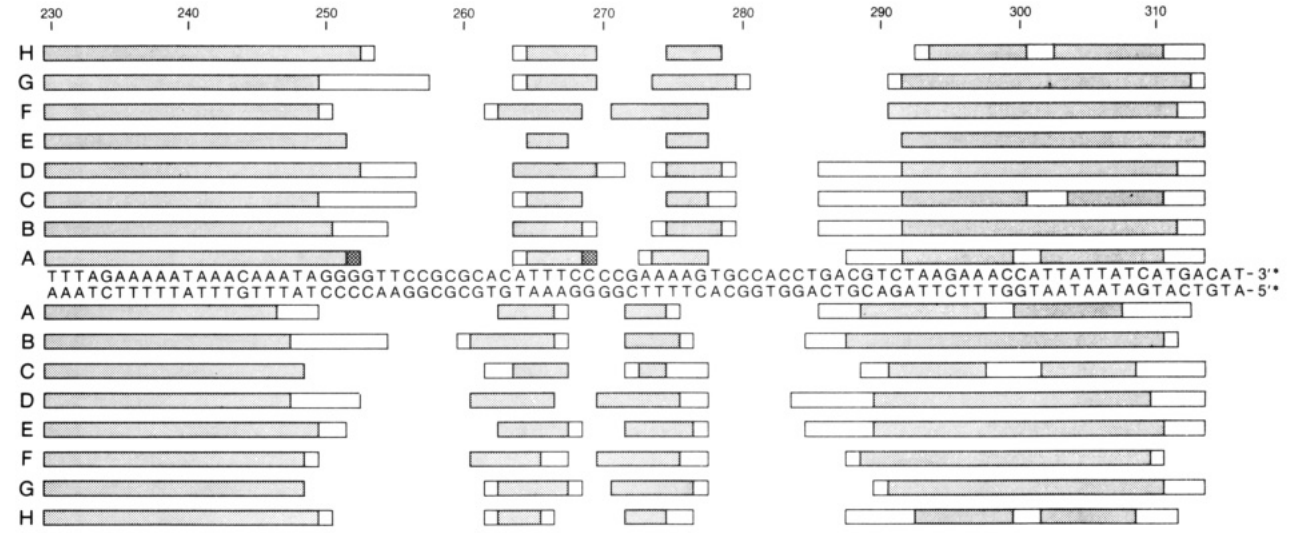

Figure 8. Footprinting pattern of the new linked bis-netropsins and distamycin on the analyzed portion of the restriction fragment studied at lower (0.16) and higher (0.78) ratio. Nonmarked region: footprint at 0.78 ratio only (not observed at 0.16 ratio). Region marked by dots: footprint consistent both at 0.16 and 0.78 ratios. Region marked by cross slashes: footprint at 0.16 ratio only (not observed at 0.78 ratio). A (**3**), B (**4**), C (**5**), D (**6**), E (**7**), F (**8**), G (**9**), and H (**2**).

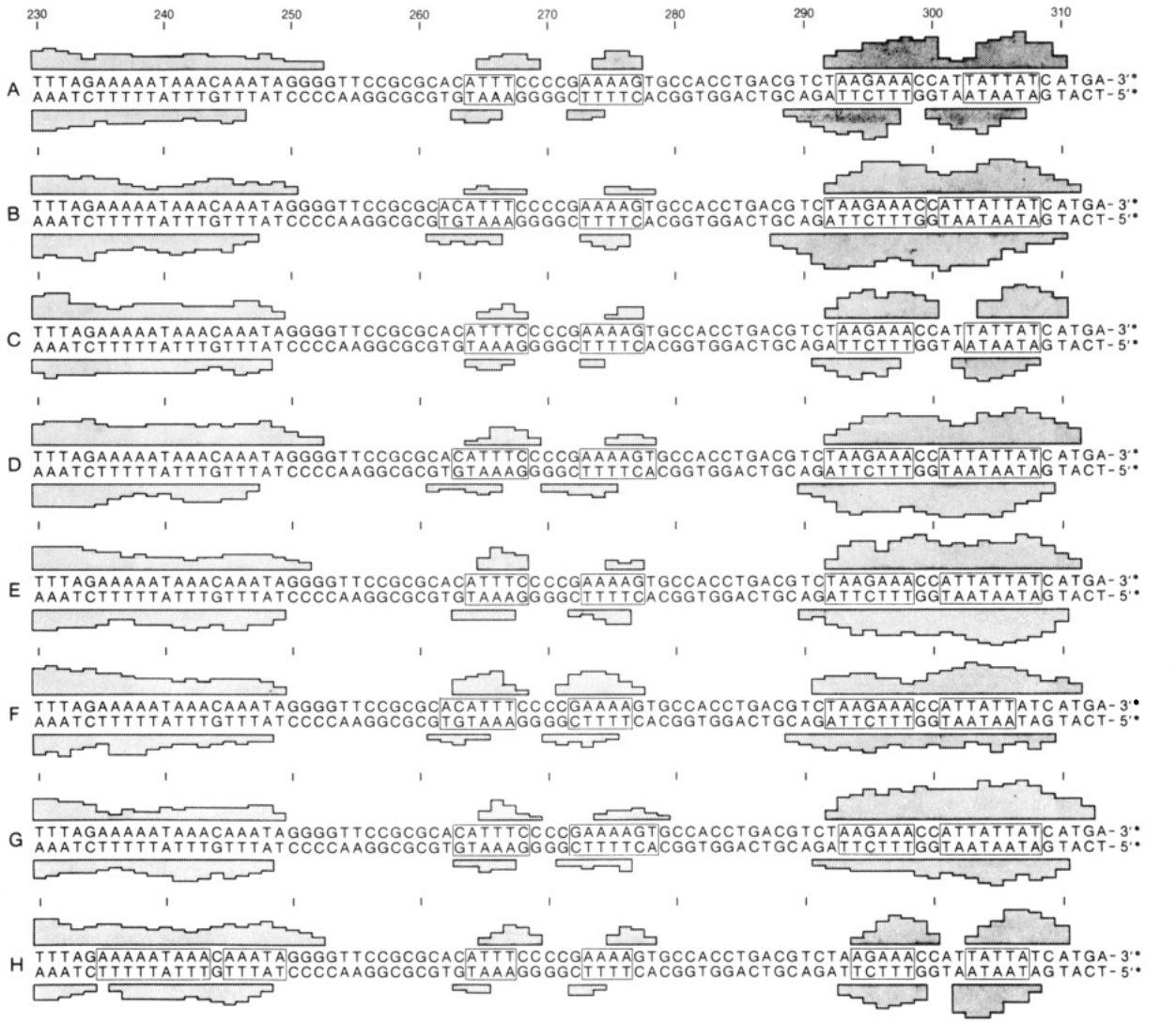

Figure 9. Footprinting of compounds **3** (A), **4** (B), **5** (C), **6** (D), **7** (E), **8** (F), **9** (G), and **2** (H) on the restriction fragment analyzed. Histogram height is proportional to the protection from the cleavage at each base pair relative to unprotected DNA (in the absence of ligands). Upper and lower footprints are from 3′- and 5′-end-labeled DNA, respectively.

0.8 Å. The MM2 calculation localizes the most stable conformation at $\zeta 1 = 130°$ and $\zeta 2 = 275°$. The conformations predicted to be suitable for bidentate binding are approximately 3 kcal higher in energy. Thus the trans three-membered ring is a relatively good tether with respect to its linker length flexibility and spatial disposition of the groups. However the fact that the most

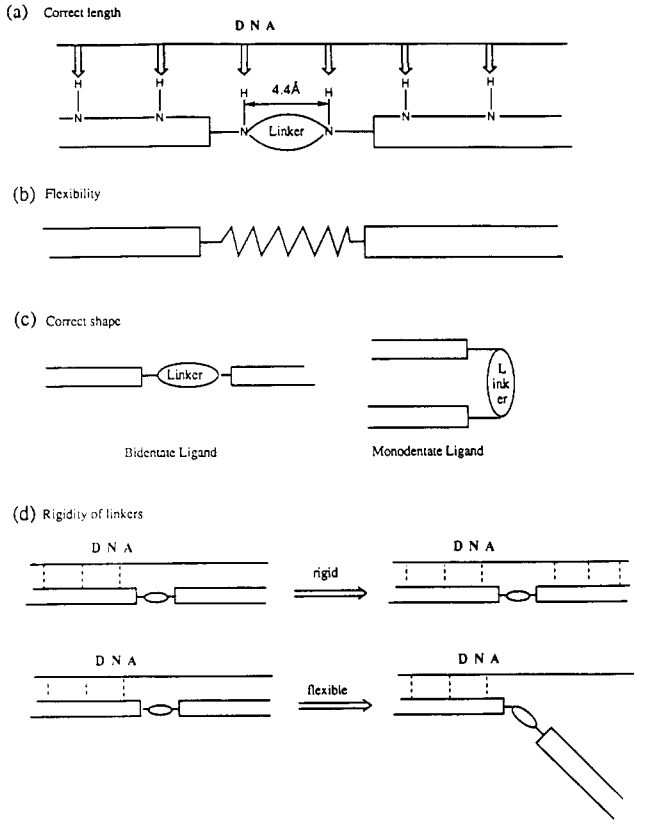

Figure 10. Depiction of a hypothetical ideal linker in terms of linker (a) length, (b) flexibility, (c) correct shape, and (d) rigidity.

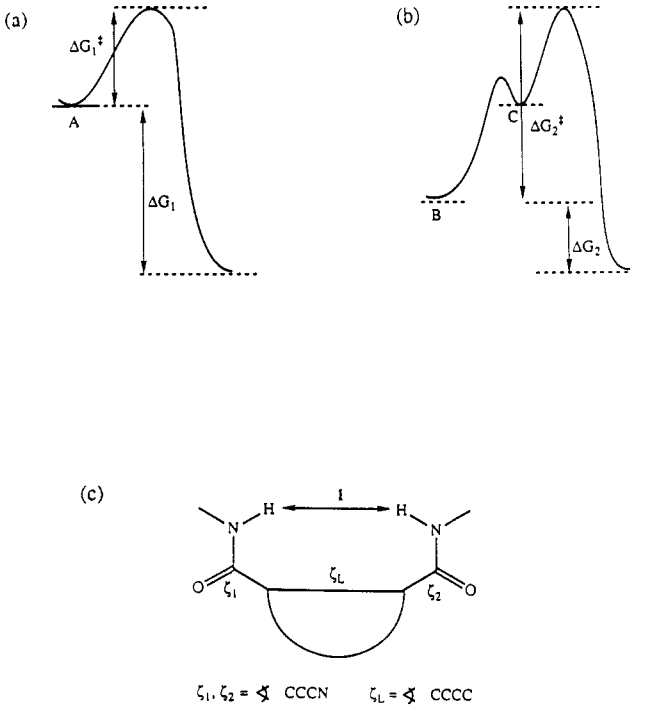

Figure 11. Representation of energy changes upon binding of a ligand to DNA (a) the case in which the ideal ligand has already adopted its most stable conformation A which is appropriate for binding to DNA, (b) the case in which the preferred conformation B must change to a less favorable one C prior to DNA binding, (c) definition of dimensions and dihedral angles employed in MMX calculations.

stable conformation cannot bind directly to the DNA without further adjustment indicates that this is not yet an ideal linker.

Cis Cyclopropane Linker. The required linker length l of 4.4 Å is found in several conformations of this tether molecule

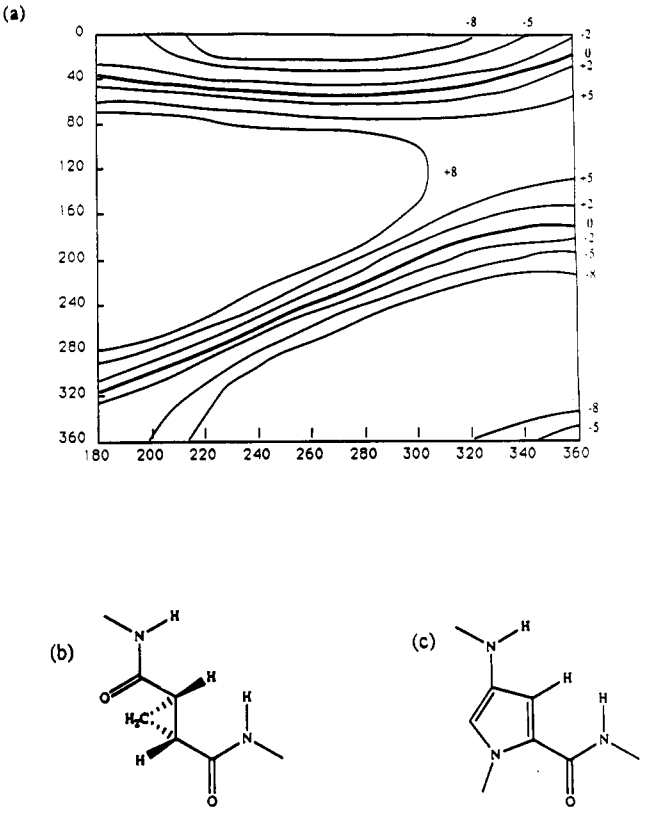

Figure 12. (a) Conformation plot for trans cyclopropane linked ligand. Contour lines represent identical repeat lengths. The following symbols were used: linker length l (symbol): 5.2 (+8), 4.9 (+5), 4.6 (+2), 4.4 (0), 4.2 (−2), 3.9 (−5), 3.6 (−8), (b) comparison of preferred conformation adopted by trans cyclopropane compound with the *N*-methylpyrrole counterpart.

(Figure 13a). However the shape of the ligand bearing two bis-pyrrole moieties joined by the tether with ζ1 = 180° and ζ2 = 0° [test iii above] resembles a propeller more than the required progressively curved conformation [Figures 13b,c (ii)]. The conformation with ζ1 = 180° and ζ2 = 180° has a spatial arrangement more suitable for binding to DNA. However the linker length is much too long (Figure 13d). The partial double bond between the nitrogen and carbon of the amide bond gives rise to the existence of two diastereomers with predominance of the s-trans configuration.[39] It is reasonable to assume that the energy gain through bidentate binding outweighs the energy required for the less stable s-cis configuration. Therefore this configuration was also considered in the analysis. The conformation plot of the s-trans, s-cis compound (Figure 14a) shows an acceptable linker length at ζ2 = 90° and 270°, respectively, and ζ1 going from 0° to 180°. However the spatial requirements for bidentate binding cannot be fulfilled by either of these conformations (Figure 14b). The shape of the s-cis–s-cis compound as well as the linker length do not permit a bidentate binding of this conformation (Figure 14c). We thus conclude that there is no conformation for this tether which has the correct linker length and the required crescent shape conformation.

This "cis-limitation" is presumably responsible for the observed monodentate binding mode of all cis compounds with ζL = 0° [cis cyclopropane, cis cyclobutane, cis double bond (vide infra)].

Trans Cyclobutane. The conformation plot is very similar to that of the corresponding three-membered ring. The linker length in suitable conformations is slightly shorter, caused by the smaller angle between the substituents and the ring (ζL = 112° vs 120° for cyclopropane). Two conformations are possible for cyclobutane, a flat planar structure or a puckered one. The energy difference between these two conformations appears to be small.[40]

(39) Deslongchamps, P. *Stereoelectronic Effects in Organic Chemistry*; Pergamon Press: Oxford, 1983.
(40) Allinger, N. L.; Tushaus, L. A. *J. Org. Chem.* **1965**, *30*, 1945.

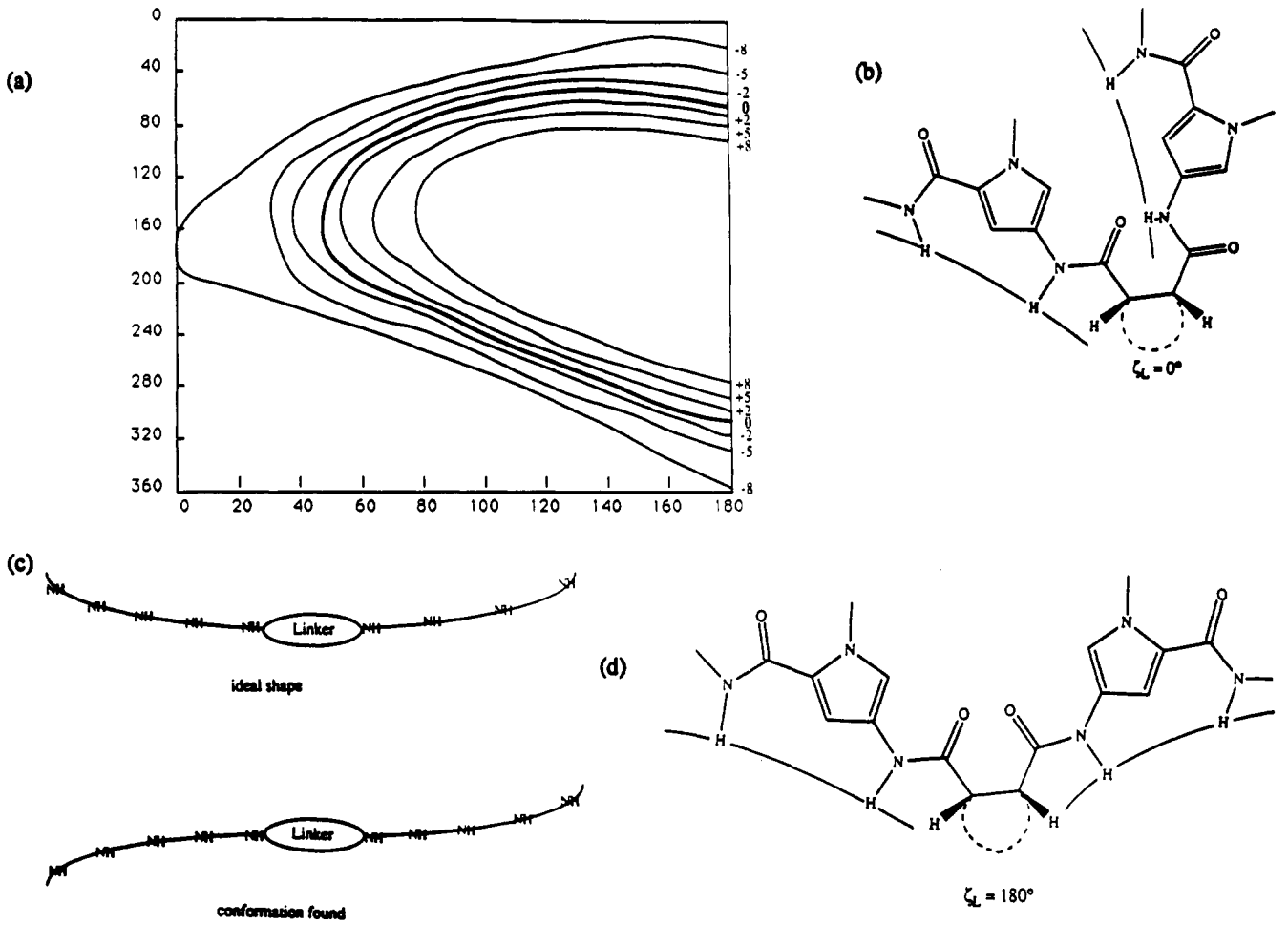

Figure 13. (a) Conformation plot for cis cyclopropane linked ligand. (b) Amide s-trans–s-trans, $\zeta 1 = 180°$, $\zeta 2 = 0°$. (c) Comparison of ideal linker shape and conformation predicted for cis cyclopropane linked ligand as depicted in b. (d) Amide s-trans–s-trans, $\zeta 1 = \zeta 2 = 180°$.

Therefore a similar binding mode to that deduced for the trans three-membered linker is expected.

Cyclohexane Derivatives. The dihedral angle ζL between the two substituents is the same for the cis and trans compound in the chair conformation. The conformation plots (figure not shown) are identical for both configurations. The torsional angle of the substituents is between that found in the cis cyclopropane derivative ($\zeta L = 0°$) and that found for the corresponding trans isomer ($\zeta L = 120°$). Therefore the shape of the backbone (amide–C–C–amide) is between these two conformations. This compromise conformation is therefore predicted to be neither a particularly good bidentate binder nor can this binding mode be completely neglected. The analysis therefore indicates a poor bidentate binding tendency, if at all, for either isomer in the chain conformation. However the boat conformation of the trans-linked compound permits binding in a bidentate fashion. The torsional angle $\zeta L = 120°$, is identical with that derived for the trans cyclopropane derivative. The conformation plots therefore resembles that for the three membered ring linker.

Again, conformations with $\zeta 1 \sim 0°$ and $\zeta 2 \sim 180°$ have the correct linker length as well as the preferred shape required for acting as a bidentate ligand. The difference between the chair and the boat conformation for the trans cyclohexane linked compound was calculated to be 7 kcal M^{-1}. This energy difference is of the same order of magnitude as the thermodynamic driving force (ΔG) for the binding of monodentate lexitropsins to B-DNA. Therefore if bidentate binding takes place at all for the trans cyclohexane compound it should be much weaker than that observed for the compound linked with the trans cyclopropane unit. The tendency for bidentate binding of the cis compound in the boat conformation is less pronounced than in the chair conformation ($\zeta L = 0°$ vs $\zeta L = 60°$).

Cyclopentane. In the envelope conformation with one substituent in the bow position the situation is similar to that of the chair conformation of the cyclohexane derivatives. Therefore, from the preceding analysis, the compounds in these conformations cannot bind strongly to DNA. Alternatively if the substituents are attached to the two ring positions located in the plane of the envelope conformation, the relative disposition of the substituents is identical with that found for the cyclohexane moiety in the boat conformation. The most stable trans conformation calculated is the half chair, with no local minima detected for the envelope conformation. The difference in energy between the conformations is much smaller than in the cyclohexane case. Substituted cyclopentane derivatives are known to exist in a shallow potential well in which rapid interconversion of conformers occurs.[41] The tendency for a bidentate binding mode of the trans cyclopentane linked structure is therefore more pronounced than for the corresponding six-membered ring, but lower compared with the trans cyclopropane derivative.

Trans Double Bond. All conformations in which $\zeta 2 = 180° = \zeta 1$ have the correct geometry for binding. The linker length is around 4.2 Å in all these conformations (Figure 15a). MM2 calculation indicates a small difference (<1 kcal M^{-1}) between the planar s-trans, s-cis conformation ($\zeta 1 = 180°$ and 0°, respectively, $\zeta 2 = 0°$ and 180°, respectively) and the most stable all s-trans compound. These parameters indicate a high probability for this compound to bind in a bidentate fashion to DNA. However the flexibility of the ligand is poor. The smallest linker length in an "allowed" conformation is about 4.2 Å. The relevant properties of this linker for minor groove binding are very similar to those of the pyrrole moiety (Figure 15b). Therefore, the binding of a compound bearing two *N*-methylpyrrole units joined by this tether should be similar to that observed for Nt-5. It has been

(41) Lambert, J. B.; Papay, J. J.; Khan, S. A.; Kappauf, K. A.; Magyars, E. S. *J. Am. Chem. Soc.* **1974**, *96*, 6112.

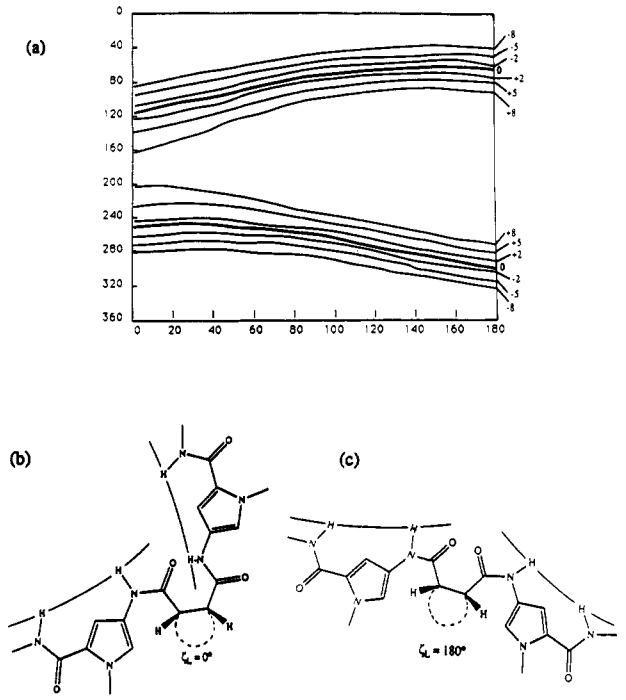

Figure 14. (a) Conformation plot of s-cis–s-trans cis cyclopropane linked ligand showing acceptable linker length at $\zeta 2 = 90°$ and 270° and for $\zeta 1$ going from 0° to 180°, respectively. (b) Amide s-cis–s-trans, $\zeta 1 = 180°$ and $\zeta 2 = 0°$. (c) Amide s-cis–s-cis, $\zeta 1 = \zeta 2 = 180°$.

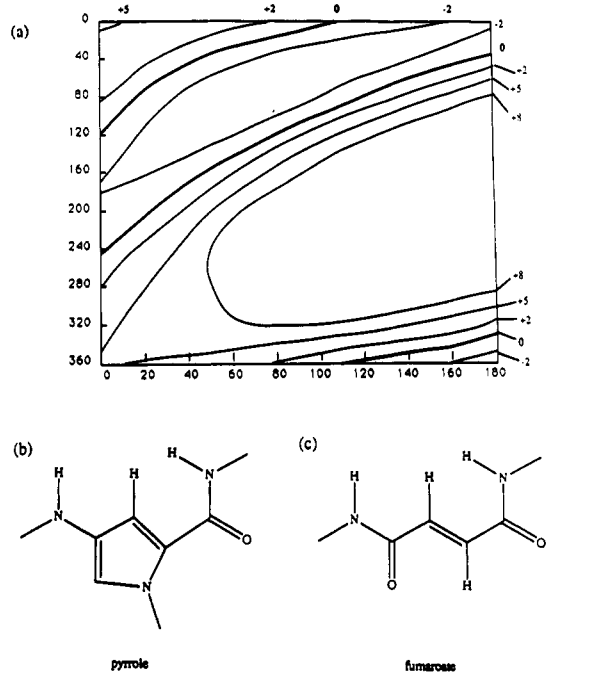

Figure 15. (a) Conformation plots for trans double bond linker. (b) Comparison of geometry of trans fumarate linker with *N*-methylpyrrole moiety.

noted that for longer ligands bearing *N*-methylpyrrole units there will be a limit beyond which these oligo(*n*-methylpyrrole)-carboxamides can no longer follow the right-handed helical twist along the minor groove of B-DNA.[42] One pyrrole unit is about 0.4 Å too long; therefore, a linker joining two pyrrole units should have a linker length of about 3.6 Å (−8). Thus the trans olefinic link cannot completely compensate for the lack of dimensional correspondence between oligonucleotides and their complementary

(42) Dervan, P. B. *Science* **1986**, *232*, 464.

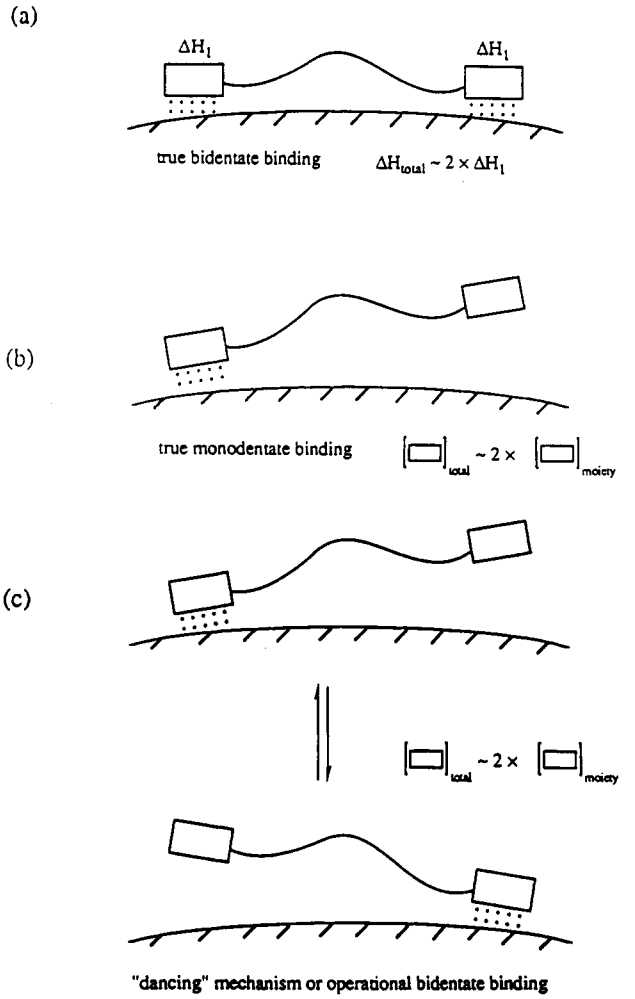

Figure 16. Depiction of alternative modes of binding of potentially bidentate ligands (a) true bidentate binding, (b) true monodentate binding, (c) dancing mechanism or operational bidentate binding.

oligopeptides. However this tether should be ideal for joining ligands which have the correct repeat length (for example 1,2,4-triazole and thiazole with nitrogen directed in to the minor groove).

Discussion

Role of Cis and Trans Linkers in Binding of the Ligands to DNA. The present compounds are designed to study the role of rigid linker with cis and trans orientations in interaction of the bis-*N*-methylpyrrole dipeptide ligands with DNA. The results suggest that the trans compound **6** binds to DNA in a bidentate fashion while its cis isomer **5** binds in a monodentate way (Figure 16). If trans compound **6** binds to DNA in a true bidentate fashion (Figure 16a), one can expect a binding constant of this compound for poly(dA-dT) significantly greater than Dst which possesses three pyrrole rings and one cationic charge. Contrary to the prediction this compound has about six times lower binding constant than Dst. Probably this observed discrepancy in K_a value of compound **6** indicates that the rigid linker is not permitting both the bis-pyrrole arms of the compound to bind firmly in the minor groove of DNA at the same time. It is plausible to conclude that a sort of "dancing" interaction mechanism could be operating in the case of compound **6** with one arm sitting on DNA firmly at a given moment (as in Figure 16c). From the observed r_b and K_a values of compound **5** it is reasonable to assume that this compound binds to DNA with only half of the molecule while the other half is positioned somewhat remote from the floor

Table II. Summary of Structural Characteristics of Alternative Linkers from Molecular Mechanics Calculations as Potential Tethers[a]

compound		shape/length	flexibility	stability	rigidity
		cyclic compounds			
cis	$n = 3$	d	-	-	-
	$n = 4$	d	-	-	-
	$n = 5$	c	b	b	b
	$n = 6$	c	b	b	b
trans	$n = 3$	b	b	b	b
	$n = 4$	b	b	b	b
	$n = 5$	b	b	b	b
	$n = 6$	b	b	c	b
		double bond			
cis		d	-	-	-
trans		a	c	a	b

[a] a = very good, b = good, c = acceptable-poor, d = unacceptable.

of the minor groove of DNA.

The footprinting patterns and particularly the binding site size of the cis-linked structures are similar to those of distamycin indicating that in these cases only one of the arms binds at a time to the DNA in a monodentate fashion as shown in Figure 16b while the second bis-pyrrole moiety is directed away from the minor groove. In contrast to the behavior of the cis compounds, the trans isomers protect longer sequences of the DNA against MPE cleavage. This may correspond to actual bidentate binding with both arms of the ligand bound to the receptor or an "operational bidentate" binding in which one arm is bound tightly and the second arm is constrained close enough to the adjacent portion of the minor groove to prevent cleavage by the footprinting agent. However the footprinting patterns of all the trans compounds are not the same. The compounds linked by trans cyclopropane, cyclobutane, and fumaroyl moieties give evidence of bidentate binding, and those compounds linked by trans cyclopentane and trans cyclohexane rings give slightly weaker and shorter footprints. These results are in accord with the molecular mechanics analyses and indicate that conformational flexibility of the linker also plays a role in interaction of the bis trans-linked compounds with DNA.

The force field analysis indicates that while none of the tested tethers appears to be ideal (Table II) several of them have useful characteristics. The better tethers amongst those examined in this study are the trans cyclopropane, trans cyclobutane, and trans cyclopentane moieties, the fumaroic acid derivative and finally the succinate bridge. However, as explained in connection with the footprinting results, it cannot be excluded that they bind to DNA only in an operational bidentate fashion (Figure 16). Thus all of the factors discussed in this analysis which favor true bidentate binding also apply to the "dancing" mechanism. Distamycin-2 binds to DNA about 10 times weaker than distamycin-3.[43] From the experimentally determined binding constants of Dst-3 (**2**), K_a for Dst-2 can be estimated to be 4×10^4 M^{-1} with a ΔG for binding of about 6.3 kcal M^{-1}. The enthalpy of bidentate binding is expected to be about twice that for monodentate binding. Provided the entropic factors are comparable for each moiety and additive (which may not be the case) a K_a of about 10^9 is expected in the ideal case.[19,20] However because of strain in the bound ligand and less efficient binding of the longer nonideal lexitropsin, the observed K_a can be lower. Regardless of the details of the molecular recognition processes the K_a for true monodentate binding and a "dancing" process should exhibit K_a about twice as large as that for Dst-2 because of the effective doubling of the concentration of the ligand. This analysis therefore indicates a dancing mode for **6** rather than true bidentate binding. A systematic analysis of thermodynamic data from microcalorimetry as well as detailed NMR experiments should permit a more reliable differentiation of the binding modes, and such studies are ongoing.

Acknowledgment. We wish to thank Dr. M. Dobler for use of the MacMOMO program and Dr. R. S. Brown for use of his microcomputer facilities.

Registry No. **1**, 1438-30-8; **2**, 636-47-5; **3**, 130699-06-8; **4**, 130699-07-9; **5**, 130699-08-0; **6**, 130699-09-1; **7**, 130699-10-4; **8**, 130699-11-5; **9**, 130699-12-6; poly(dA-dT), 26966-61-0; lexitropsin, 121854-21-5.

Supplementary Material Available: Conformation plots of all the compounds studied in this paper (12 pages). Ordering information is given on any current masthead page.

(43) Zimmer, Ch.; Luck, G.; Birch-Hirschfeld, E.; Weiss, R.; Arcamine, E.; Guschlbauer, W. *Biochim. Biophys. Acta* **1983**, *741*, 15.

Design of α-Alkyl β-Hydroxy Esters Suitable for Providing Optical Resolution by Lipase Hydrolysis

Toshiyuki Itoh,* Keiko Kuroda, Miki Tomosada, and Yumiko Takagi

Department of Chemistry, Faculty of Education, Okayama University, Okayama 700, Japan

Received February 26, 1990

A study of the lipase-catalyzed hydrolyses of various α-substituted β-acetoxy esters revealed that a sulfur functional group in the ester, which could play an important role in the stereorecognition by lipase A6 (*Aspergillus* sp.) and an anti conformation in the ester, promotes satisfactory results in the hydrolysis.

Optically active 3-hydroxy ester derivatives are now widely recognized as highly useful chiral building blocks in the syntheses of many optically active natural and unnatural products.[1] Recently, many commercially available

0022-3263/91/1956-0797$02.50/0 © 1991 American Chemical Society